NOTICE

**PORTIONS OF THIS REPORT ARE ILLEGIBLE.** It has been reproduced from the best available copy to permit the broadest possible availability.

HEDL-SA-789

CONF-750607--48

# $Eu_2O_3$ and $B_4C$ Worth Calculations in Fast Reactor Spectra

J. W. Daughtry

MASTER

To be presented at the 1975 Annual Meeting of the American Nuclear Society, June 8-13, 1975, Marriott Hotel, New Orleans, Louisiana.

Hanford Engineering Development Laboratory, Richland, Washington, operated by Westinghouse Hanford Company, a subsidiary of Westinghouse Electric Corporation, for the United States Energy Research and Development Administration under contract number AT(45-1)-2170.

NOTICE

This report was prepared as an account of work sponsored by the United States Government. Neither the United States nor the United States Energy Research and Development Administration, nor any of their employees, nor any of their contractors, subcontractors, or their employees, makes any warranty, express or implied, or assumes any legal liability or responsibility for the accuracy, completeness or usefulness of any information, apparatus, product or process disclosed, or represents that its use would not infringe privately owned rights.

DISTRIBUTION OF THIS DOCUMENT IS UNLIMITED

## DISCLAIMER

This report was prepared as an account of work sponsored by an agency of the United States Government. Neither the United States Government nor any agency thereof, nor any of their employees, makes any warranty, express or implied, or assumes any legal liability or responsibility for the accuracy, completeness, or usefulness of any information, apparatus, product, or process disclosed, or represents that its use would not infringe privately owned rights. Reference herein to any specific commercial product, process, or service by trade name, trademark, manufacturer, or otherwise does not necessarily constitute or imply its endorsement, recommendation, or favoring by the United States Government or any agency thereof. The views and opinions of authors expressed herein do not necessarily state or reflect those of the United States Government or any agency thereof.

---

## DISCLAIMER

Portions of this document may be illegible in electronic image products. Images are produced from the best available original document.

## 1. INTRODUCTION

Work is now in progress to design and fabricate europia ($Eu_2O_3$) control rods for irradiation testing in one of the early operating cycles of the Fast Test Reactor (FTR). These tests will provide data for evaluating europia as a possible control rod absorber material in fast reactors. Prediction of the reactivity worth of the europia rods is a necessary part of the design process. To improve the accuracy of these predictions, an experiment was performed in the FTR Engineering Mockup Critical (EMC) to determine the relative reactivity worth of $Eu_2O_3$ and boron carbide ($B_4C$) in control rod size quantities. Upon completion of the experiment, calculations were performed to obtain reactivity worths for comparison with the measured worths. From this comparison, calculation-vs.-experiment (C/E) bias factors were obtained for use in correcting the computed reactivity worth of europia in the FTR.

This report gives a brief description of the experiment (a detailed description is available in the references), the experimental results, a description of the analytical methods, the calculated results, and a comparison of the calculated and experimental results. Also included are discussions of the effects of resonance self-shielding and mesh spacing on computed absorber rod worths.

## 2. BACKGROUND INFORMATION

The initial FTR core will have natural boron carbide ($B_4C$) control rods. Other absorber materials have been considered primarily as a backup to the $B_4C$ rods. Studies were conducted to evaluate tantalum (Ta) as a possible control material. However, Ta was found to be unsuitable primarily due to gamma heating problems. The isotopic composition of tantalum is greater than 99.9% $^{181}Ta$. Absorption of neutrons produces $^{182}Ta$ which has a half life of 115 days. The gamma activity associated with the decay of $^{182}Ta$ is sufficiently high that gamma heating would present cooling problems during refueling and other shutdown operations.

Another absorber material that has been considered for use in fast reactors is europia (europium oxide, $Eu_2O_3$). Europia is attractive because its worth is comparable to that of boron carbide on an equal volume basis and it

does not produce helium. Furthermore, neutron capture by either of the naturally occurring isotopes of europium, $^{151}Eu$ and $^{153}Eu$, produces isotopes that also have relatively high neutron capture cross sections. This effect could result in a significant increase in the useful lifetime of a europia control rod.

In anticipation of the possible use of europia in liquid metal cooled fast breeder reactors (LMFBRs) and in the FTR, calculations were performed by Hanford Engineering and Development Laboratory (HEDL) personnel to determine the relative worth of boron carbide and europia. The results of the study were not in agreement with experimental data. A review of europium cross section data showed large differences in the measured capture cross sections reported by different experimenters. It was concluded that the knowledge of the europium cross section was not sufficient to properly assess the merits of europia relative to boron carbide. Consequently, in January 1973 HEDL proposed that a set of experiments be performed in the FTR-EMC to obtain integral data on the relative worth of europia and boron carbide in control rod-size quantities. The Division of Reactor Development and Technology (RDT) of the Atomic Energy Commission (AEC), now the Energy Research and Development Administration (ERDA), concurred with the HEDL proposal and directed HEDL to coordinate efforts to define and accomplish the appropriate experiment in the FTR-EMC. Concurrently, RDT directed Argonne National Laboratory (ANL), to take the necessary action to procure and fabricate the europia required for the conduct of the experiment.

A set of measurements to obtain the desired information was defined by HEDL and the experimental requirements were transmitted to ANL in April 1973. Based on these requirements ANL prepared detailed plans for the europia worth experiment to be conducted in FTR-EMC.

In the meantime, ANL procured the necessary europia and arranged for fabrication of the material into platelets suitable for use in the zero power critical facilities.

After final concurrence in the experimental plans and delivery of the fabricated $Eu_2O_3$ plates, the experiment was conducted in the FTR-EMC in September and October 1973.

Preliminary data from the experiments was transmitted to HEDL by ANL during the experiment and immediately after completion of the experiment. A final report on the europia worth experiment was transmitted to HEDL by ANL in January 1974.

## 3. DESCRIPTION OF THE EXPERIMENT

The EMC experiments for the FTR were performed by personnel of the Applied Physics Division of Argonne National Laboratory in the ZPR-9 critical facility. Initial criticality of the FTR-EMC was achieved in March 1971. For a detailed description of the mockup, see References 1 and 2.

The program of experiments performed in the EMC was divided into two phases. The first phase, designated Phace C of the FFTF critical experiments program[3], was composed of experiments related to core and shielding design and to safety problems having direct impact on the design. The second phase of experiments, designated Phase D, consisted of measurements related to FFTF operations and safety.

The europia worth experiment was Part IV of Phase D. The purpose of the experiment was to evaluate the control properties of europia in a fast reactor environment. There were three specific objectives: (1) to compare the worth of europia with that of boron carbide on an equal volume basis, (2) to investigate self-shielding effects, and (3) to provide a basis for the evaluation of analytical methods for computing $B_4C$ and $Eu_2O_3$ control rod worths and for the evaluation of europium cross section data.

A description of the reactor configuration for this experiment, the measurements that were made, and the results obtained are given, briefly, below. For further details see Reference 4.

### 3.1 Reference Core Configuration

The reference configuration for the experiment was designated BOL-REF-5S. It was an EMC configuration representing the FTR at the beginning-of-life. Figure 1 is a diagram showing the BOL-REF-5S configuration of the EMC as viewed at the midplane of the assembly. At the bottom right is a region added to the EMC for other experiments, representing a portion of the FTR

radial shield. The simulated peripheral shim, PSR-722 (shown with a dashed outline), was not part of the BOL-REF-5S configuration but is shown because it was one of the three locations at which europia worth measurements were made. In the BOL-REF-5S configuration the three simulated safety rods, SR-304, SR-308, and SR-312 were parked. A parked rod is one that is withdrawn 36" so that the absorber material is above the core, the bottom tip of the absorber is even with the top of the core and the safety rod channel is filled with sodium. Of the six control rods, CR-506, CR-514, and CR-522 were parked and CR-508, CR-516 and CR-524 were fully inserted. The excess reactivity of BOL-REF-5S configuration was measured on six different occasions from August 1973 to June 1974. The excess reactivity decreased gradually with time due to the radioactive decay of $^{241}Pu$. Over a time span of this duration the decay of $^{241}Pu$ can be adequately approximated by a straight line. A least squares fit of the excess reactivity data to a straight line (see Appendix A) provided a curve of the excess reactivity of the BOL-REF-5S configuration at any time during the Phase D experiments. The excess reactivity of this reference configuration was between 80 and 100 inhours during the europia experiment.

### 3.2 Description of Absorber Assemblies

Europia and boron carbide worth measurements were made at three locations in the EMC: (1) the simulated row 3 safety rod location, SR-308, (2) the simulated row 5 control rod location, CR-514, and (3) the simulated row 7 peripheral shim rod location, PSR-722 (see Figure 1). In order to investigate self-shielding effects, four control material compositions were employed for both europia and boron carbide. The four europia platelet loading patterns are shown in Figure 2. Each simulated absorber rod (control, safety, or peripheral shim) was an array of four matrix tubes, two type A and two type B, arranged as indicated in Figure 3.

The diagrams in Figure 2 show the arrangement of sodium (Na) and europia ($Eu_2O_3$) within each matrix tube. The overall length of the absorber region of a simulated rod was 91.6 cm. The total volume of this length of four matrix tubes was 11.209 liters.

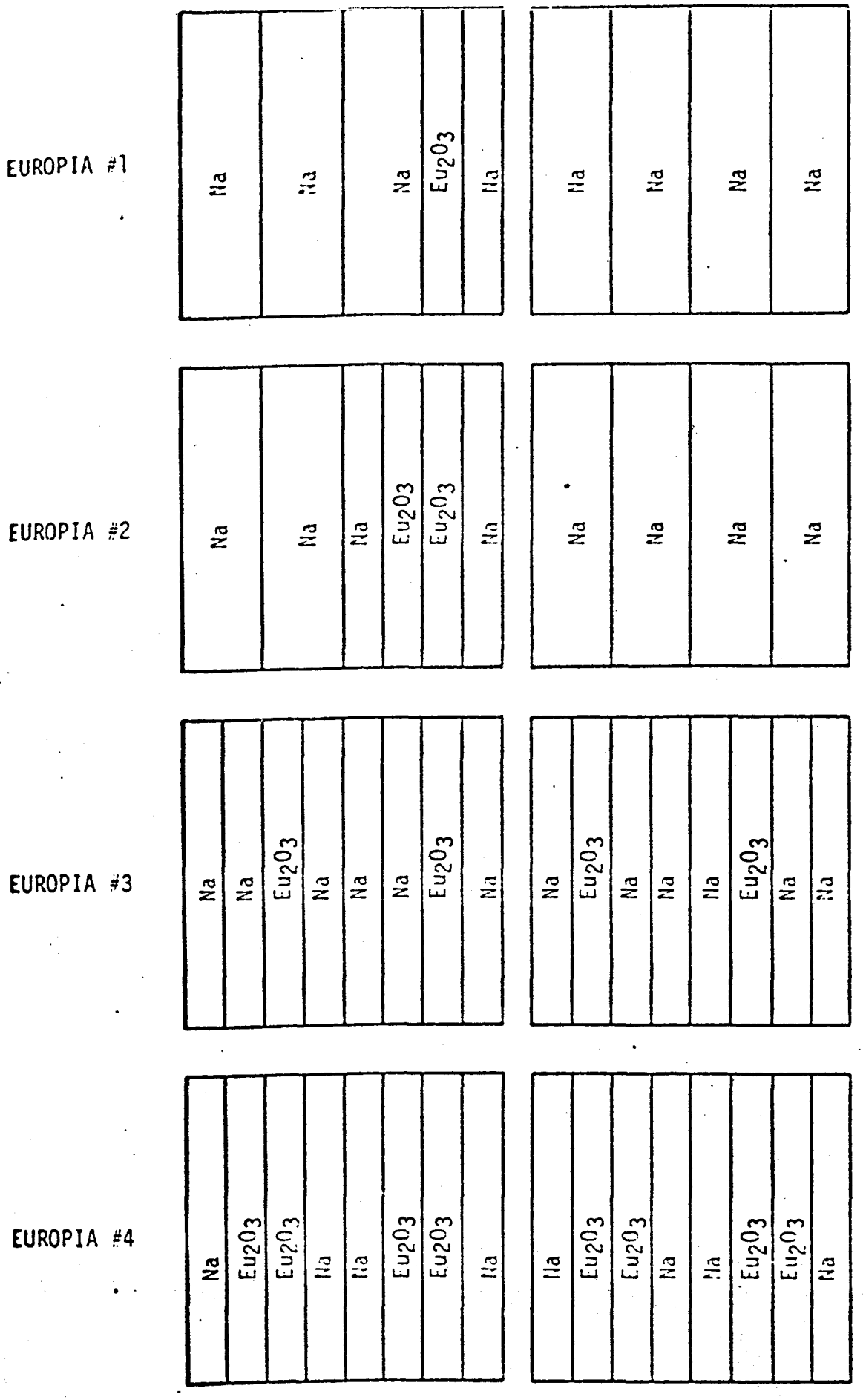


HEDL 7502-086.8

**Figure 2.** Europia Control Material Loading Patterns

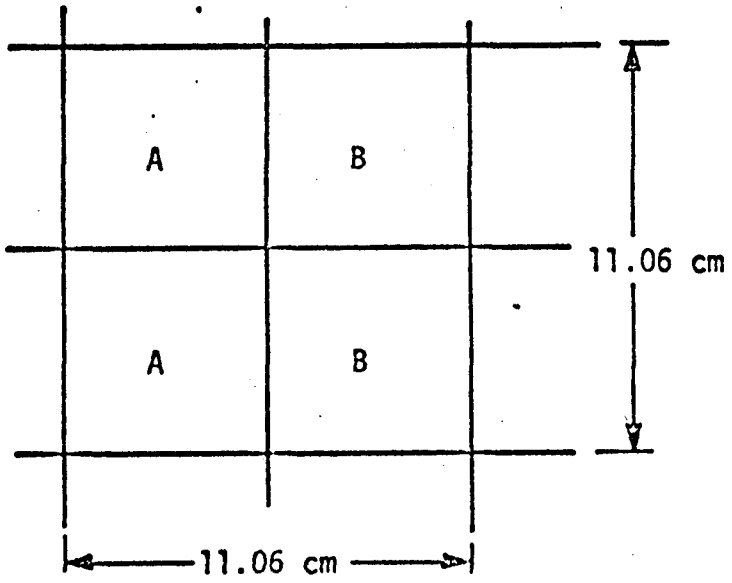


Figure 3. Arrangement of Type A and Type B Tubes in a Simulated Absorber Rod

Table I. Atom Densities of $Eu_2O_3$, $B_4C$ and Sodium Channel Compositions

$10^{21}$ atoms/cm$^3$

| Isotope or Element | $Eu_2O_3$ Compositions[a] | | | | $B_4C$ Compositions[b] | | | | Sodium Channel Composition |
|---|---|---|---|---|---|---|---|---|---|
| | #1 | #2 | #3 | #4 | #1 | #2 | #3 | #4 | |
| $^{151}Eu$ | 0.4511 | 0.9022 | 1.7993 | 3.6010 | | | | | |
| $^{153}Eu$ | 0.4862 | 0.9724 | 1.9392 | 3.8810 | | | | | |
| Fe | 10.9398 | 11.3193 | 13.7504 | 13.5933 | 10.8920 | 11.2226 | 13.5550 | 13.2067 | 10.5612 |
| Ni | 1.4544 | 1.5104 | 1.8690 | 1.8459 | 1.4472 | 1.4960 | 1.8400 | 1.7884 | 1.3985 |
| Cr | 3.1274 | 3.2367 | 3.9367 | 3.8914 | 3.1135 | 3.2086 | 3.8800 | 3.7793 | 3.0184 |
| Mn | 0.2406 | 0.2487 | 0.3010 | 0.2976 | 0.2396 | 0.2467 | 0.2968 | 0.2892 | 0.2325 |
| Mo | 0.0099 | 0.0099 | 0.0099 | 0.0099 | 0.0099 | 0.0099 | 0.0099 | 0.0099 | 0.0099 |
| C | 0.0316 | 0.0323 | 0.0362 | 0.0360 | 0.8063 | 1.5710 | 3.1258 | 6.1705 | 0.0310 |
| Si | 0.1977 | 0.2045 | 0.2482 | 0.2454 | 0.1969 | 0.2028 | 0.2447 | 0.2384 | 0.1909 |
| Cu | 0.0212 | 0.0218 | 0.0255 | 0.0253 | 0.0211 | 0.0216 | 0.0252 | 0.0247 | 0.0206 |
| S | 0.0021 | 0.0021 | 0.0027 | 0.0027 | 0.0020 | 0.0021 | 0.0027 | 0.0026 | 0.0020 |
| P | 0.0056 | 0.0057 | 0.0067 | 0.0066 | 0.0056 | 0.0057 | 0.0066 | 0.0065 | 0.0054 |
| Co | 0.0092 | 0.0093 | 0.0104 | 0.0103 | 0.0091 | 0.0093 | 0.0103 | 0.0101 | 0.0090 |
| Aℓ | 0.0062 | 0.0068 | 0.0103 | 0.0101 | 0.0061 | 0.0066 | 0.0100 | 0.0095 | 0.0057 |
| Na | 17.2426 | 15.9569 | 12.3632 | 8.2421 | 17.2426 | 15.9569 | 12.3632 | 8.2421 | 18.5284 |
| O | 1.4060 | 2.8119 | 5.6075 | 11.2228 | 0.0008 | 0.0015 | 0.0031 | 0.0061 | |
| H | | | | | 0.0123 | 0.0245 | 0.0491 | 0.0976 | |
| N | | | | | 0.0027 | 0.0053 | 0.0106 | 0.0211 | |
| $^{10}B$ | | | | | 0.5786 | 1.1494 | 2.3079 | 4.5826 | |
| $^{11}B$ | | | | | 2.3780 | 4.7240 | 9.4852 | 18.8338 | |

[a] Isotopic composition of $Eu_2O_3$: $^{151}Eu$ 41.28 w/o; $^{153}Eu$ 45.08 w/o; O 13.64 w/o.

[b] Isotopic composition of $B_4C$: $^{10}B$ 14.00 w/o; $^{11}B$ 63.25 w/o; C 22.48 w/o; N, Fe, O, H 0.20 w/o.

+ 0.0658 ± .0039 % Δk/k. At the CR-514 location the worth was + 49.9 ± 4.3 Ih or + 0.0476 ± .0041 % Δk/k.

### 3.3.2 $B_4C$ and $Eu_2O_3$ Rod Worths

The experimental data from the $B_4C$ and $Eu_2O_3$ worth measurements are given in Table II. For each measurement of $B_4C$ worth the number of grams of $^{10}B$ and the kilograms of $B_4C$ are shown. The volume fractions were obtained by dividing the number of kilograms of $B_4C$ by the mass that would occupy the 11.208 liter control rod at the theoretical maximum density of $B_4C$ - 2.518 grams/cm$^3$ (6,7).

In the set of data for $B_4C$ at the CR-514 location one additional measurement is included. This is the worth of the EMC control rod composition, which has about 50% more boron carbide than $B_4C$ #4. The data were obtained from the control rod interaction experiment(8). In order to make this result consistent with the other measured worths in the table, two adjustments were necessary. First, the core configuration was slightly different and calculations indicated that the worth should be reduced by 1.5% to account for this difference. Second, the worth of the rod was measured for withdrawal from inserted to parked. Therefore, to be consistent with the remainder of the worth measurements in the table, the worth of removing the parked rod was added to the reported worth. The adjusted worth is given in Table II.

The europia worth data are given in Part B of Table II. The theoretical maximum density of $Eu_2O_3$ that was used to obtain the volume fractions was 7.951 grams/cm$^3$(9).

As indicated in Section 3.2, the results given in Table II are the reactivity worths of each absorber composition relative to sodium channel composition.

The worth of $B_4C$ and $Eu_2O_3$ as a function of volume fraction at the PSR-722 location is shown in Figure 4. The corresponding data at the CR-514 location are shown in Figure 5. The shaded region in each figure between 0.28 and 0.32 on the volume fraction scale corresponds to the amount of $B_4C$ in an FTR absorber rod. A range is indicated because the

## Table II

### Measured Reactivity Worths of $B_4C$ and $Eu_2O_3$ Compositions

A. $B_4C$ Worths

| Control Rod Location | $B_4C$ Composition No. | Mass of $^{10}B$ Grams | Mass of $B_4C$ kg | Volume[b] Fraction | Measured Worth Inhours[c] | Measured Worth % $\Delta k/k$[d] |
|---|---|---|---|---|---|---|
| PSR-722 | 1 | 109 | 0.769 | 0.0272 | - 50.6 ± 3.4 | -0.0483 ± .0032 |
| PSR-722 | 2 | 216 | 1.527 | 0.0541 | - 75.2 ± 3.4 | -0.0718 ± .0032 |
| PSR-722 | 3 | 434 | 3.066 | 0.1086 | - 107.5 ± 3.4 | -0.1025 ± .0032 |
| PSR-722 | 4 | 862 | 6.087 | 0.2157 | - 154.9 ± 3.4 | -0.1478 ± .0032 |
| CR-514 | 1 | 109 | 0.769 | 0.0272 | - 206.5 ± 3.4 | -0.1971 ± .0032 |
| CR-514 | 2 | 216 | 1.527 | 0.0541 | - 369.3 ± 3.5 | -0.3525 ± .0033 |
| CR-514 | 3 | 434 | 3.066 | 0.1086 | - 632.9 ± 4.8 | -0.6041 ± .0046 |
| CR-514 | 4 | 862 | 6.087 | 0.2157 | -1021.7 ± 3.4 | -0.9752 ± .0032 |
| CR-514 | a | 1324 | 9.348 | 0.3312 | -1355.6 ± 18.3 | -1.2939 ± .0175 |
| SR-308 | 4 | 862 | 6.087 | Q.2157 | -1492.3 ± 12.8 | -1.4243 ± .0123 |

B. $Eu_2O_3$ Worths

| Location | $Eu_2O_3$ Composition No. | Mass of $Eu_2O_3$ kg | Volume[b] Fraction | Measured Worth Inhours[c] | Measured Worth % $\Delta k/k$[d] |
|---|---|---|---|---|---|
| PSR-722 | 1 | 3.062 | 0.0344 | - 66.0 ± 3.4 | -0.0630 ± .0032 |
| PSR-722 | 2 | 6.125 | 0.0687 | - 93.3 ± 3.4 | -0.0891 ± .0032 |
| PSR-722 | 3 | 12.214 | 0.1371 | - 123.7 ± 3.4 | -0.1181 ± .0032 |
| PSR-722 | 4 | 24.445 | 0.2743 | - 173.7 ± 3.4 | -0.1658 ± .0032 |
| CR-514 | 1 | 3.062 | 0.0344 | - 290.0 ± 3.5 | -0.2768 ± .0033 |
| CR-514 | 2 | 6.125 | 0.0687 | - 477.4 ± 3.5 | -0.4557 ± .0033 |
| CR-514 | 3 | 12.214 | 0.1371 | - 768.9 ± 5.0 | -0.7339 ± .0048 |
| CR-514 | 4 | 24.445 | 0.2743 | -1168.3 ± 8.8 | -1.1151 ± .0084 |
| SR-308 | 4 | 24.445 | 0.2743 | -1700.8 ± 16.4 | -1.6233 ± .0157 |

a From Ref. 8 adjusted for parked rod worth.

b Based on theoretical maximum density of 2.518 g/cm$^3$ for $B_4C$ and 7.951 g/cm$^3$ for $Eu_2O_3$ and 11.208 liter control rod volume.

c From Ref. 4 except as indicated in (a).

d 1047.71 inhours = 1% $\Delta k/k$ (Ref. 5).

rods have not yet been fabricated and the amount of $B_4C$ can vary by the amount shown and still meet purchase specifications.

## 4. CALCULATIONS

The reactivity worths of the $B_4C$ and $Eu_2O_3$ substitutions were computed for comparison with the experimental results. The purpose of the computations and comparison was to evaluate the analytical methods and europia cross sections and to obtain bias factors to use for adjusting the computed worths of europia rods in the FTR.

An outline of the computational procedure is shown schematically in Figure 6. Each step in this procedure will be discussed below. The reactivity worth ($\Delta\rho$) of each absorber composition was obtained from the difference in $k_{eff}$ between the rod-in and rod-out configurations, as follows:

$$\Delta\rho = \rho_2 - \rho_1 = \frac{k_2-1}{k_2} - \frac{k_1-1}{k_1} = \frac{k_2-k_1}{k_2k_1} \quad , \tag{1}$$

where the k's are the computed eigenvalues.

### 4.1 Multigroup Cross Section Preparation

#### 4.1.1 Europium Cross Section Data Evaluations

One of the objectives of this study was to compare the computed reactivity worths of europia control rods obtained from different sources of microscopic cross section data and to determine, if possible, which source of data is preferable. Europium cross sections from three sources were compared: (1) ENDF/B version 3[10], (2) an evaluation by Schadel and Schenter[11], and (3) ENDF/B version 4[12]. In this study these three Eu evaluations are designated Eu-A, Eu-D, and Eu-H, respectively. Figure 6 shows the steps involved in the preparation of a 30-energy group cross section set from ENDF/B version 3 (Eu-A). The other two europium data evaluations were treated in the same manner and europia control rod worths were computed using each set of europium cross sections.

The platelet loading patterns for the $B_4C$ rods were identical to those in Figure 2 with the $Eu_2O_3$ replaced with $B_4C$.

The atom densities of the eight control compositions are given in Table I. The reactivity worths of all eight compositions were measured at the CR-514 and PSR-722 locations. At the SR-308 location only the worths of $Eu_2O_3$ #4 and $B_4C$ #4 were measured.

Before substituting the europia and boron carbide compositions in SR-308 or CR-514, the parked rod at each location was removed and replaced with materials representing the control rod plenum and drive shaft which are normally in the region above a simulated inserted control rod. The reactivity of the EMC was measured with each of the parked rods removed to provide the reference reactivity values needed in determining the worth of each absorber composition in SR-308 and CR-514. At the PSR-722 location a reactivity measurement was made with PSR-722 inserted but with the control rod composition removed and replaced with sodium channel composition to provide a reference for the absorber worths at that location. Thus, all boron carbide and europia worth measurements in this experiment were relative to sodium channel composition. The atom densities for sodium channel composition are given in Table I and the platelet loading was identical to the type B tubes shown for Europia #1 or #2 in Figure 2.

### 3.3 Results of the Experiment

The reactivity worths obtained in this experiment were reported in Reference 4 in units of inhours. The results are given in this section for easy reference and have also been converted to units of % $\Delta k/k$ for comparison with the calculated reactivities. The conversion factor was 1047.71 inhours per 1% $\Delta k/k$[5].

#### 3.3.1 Removal of Parked Rods

As mentioned in Section 3.2, the parked rods of SR-308 and CR-514 were removed before the $Eu_2O_3$ and $B_4C$ worth measurements were made at each location. Data were taken to give the worth of removing each parked rod and replacing it with control rod plenum and drive shaft compositions. At the SR-308 location this worth was + 68.9 ± 4.1 Ih.

### 4.1.2 ETOX Processing

Natural europium is 47.8 atom percent $^{151}Eu$ and 52.2 atom percent $^{153}Eu$. Microscopic cross section data for both isotopes were available from each of the three evaluations mentioned in the previous section. The microscopic data were processed using the ETOX code[13] to provide multigroup data in the "Russian" or Bondarenko[14] format. The ETOX code provided "infinitely dilute" group cross sections, inelastic transfer matrices. and tables of self-shielding factors as a function of temperature and $\sigma_0$ (see Appendix B).

### 4.1.3 Cross Section Libraries and Group Structure

Two multigroup, neutron cross section libraries, FTR Set 300[15] and FTR Set 300-S[16], have been employed for the analysis of the EMC experiments. Set 300 is a 30-energy group library generated from ENDF/B version 2 data but modified to be essentially equivalent to an ENDF/B version 3 set. Set 300-S is a 42-energy group library developed primarily for shielding calculations. The cross section data contained in the 25 highest energy groups (10 MeV to 275.4 eV) of cross section sets 300 and 300-S are identical. However, the energy range between 275.4 eV and thermal neutron energies is divided into four groups in Set 300 and 12 groups in Set 300-S. Europium-151 and -153 cross section data from Eu-A, Eu-D and Eu-H were prepared in 30 groups with the ETOX code and added to FTR Set 300 using PUPX, a code that prepares cross section data tapes from the ETOX output in the format needed by the HEDL reactor neutronics codes. In addition, the europium cross sections were prepared in 42 groups and added to FTR Set 300-S. The 30-group cross sections were used for the SR-308 and CR-514 worth calculations.

However, at the PSR-722 location, a comparison of the computed worth of the europia #4 composition in 30 groups and 42 groups showed that the 42-group calculations gave a worth 3% greater than that obtained in 30 groups. As a result all subsequent calculations of absorber worths at the PSR-722 location were done in 42 groups.

Infinitely dilute $^{151}Eu$ neutron capture and total cross sections in 42 groups are listed in Table III for Eu-A, Eu-D, and Eu-H. The corresponding cross sections for $^{153}Eu$ are listed in Table IV. Table V gives the energy and lethargy structure for the 42-group cross section set.

### 4.1.4 Eu Resonance Self-Shielding

Resonance self-shielding in the europia platelets was investigated to determine the best method to obtain effective cross sections for computing the worths of the four europia compositions employed in this study (see Appendix B). The investigation of this effect showed that resonance self-shielding was significant in the europia platelets; i.e., "infinitely dilute" europium cross sections would give computed europium reaction rates and worths that would be too high.

Several approximations were considered for determining the proper self-shielding effect. The "isolated lump" approximation seemed best suited for the europia #1 and #2 platelet configurations. For europia #3 and #4 the self-shielding should be greater than the isolated lump case but less than in an "infinite heterogeneous medium" of platelets with the europia #3 and #4 spacing. It was found that there was no significant difference between the computed europia worths obtained with the "isolated lump" and the "infinite heterogeneous medium" cross sections. Furthermore, the same reactivity values were obtained when homogeneously resonance self-shielded cross sections were used.

In summary, resonance self-shielding effects were found to be important but not very sensitive to the different approximations considered. The cross sections used for the calculation of europia worths were shown to be equivalent to those obtained by using homogeneous resonance self-shielding of the europia #4 composition.

### 4.1.5 One-Dimensional Model for Elastic "Down-Scattering" Cross Sections

In order to obtain effective cross sections for the transfer of neutrons from one energy group to the next lower energy (i.e., "down-scattering"), it is necessary to know the neutron spectrum. A one-

## Table III

Eu-151 Capture and Total Infinitely Dilute Neutron Cross Sections

| Group No. | $\sigma_c$, barns | | | $\sigma_t$, barns | | |
|---|---|---|---|---|---|---|
| | Eu-A | Eu-D | Eu-H | Eu-A | Eu-D | Eu-H |
| 1 | .014 | .018 | .005 | 4.835 | 4.839 | 4.828 |
| 2 | .021 | .047 | .031 | 5.407 | 5.432 | 5.398 |
| 3 | .041 | .115 | .201 | 6.507 | 6.582 | 6.490 |
| 4 | .090 | .270 | .457 | 7.317 | 7.497 | 6.733 |
| 5 | .197 | .443 | .687 | 7.508 | 7.754 | 6.947 |
| 6 | .252 | .624 | .762 | 7.689 | 8.061 | 7.524 |
| 7 | .336 | .819 | .864 | 8.097 | 8.580 | 8.136 |
| 8 | .452 | 1.110 | .961 | 8.321 | 8.979 | 8.624 |
| 9 | .720 | 1.500 | 1.169 | 8.772 | 9.552 | 9.594 |
| 10 | 1.207 | 1.990 | 1.407 | 9.504 | 10.287 | 11.136 |
| 11 | 1.863 | 2.630 | 1.678 | 10.515 | 11.282 | 12.911 |
| 12 | 2.508 | 3.470 | 2.238 | 11.677 | 12.639 | 15.130 |
| 13 | 3.589 | 4.580 | 3.327 | 13.049 | 14.040 | 17.017 |
| 14 | 4.691 | 5.660 | 4.564 | 14.353 | 15.322 | 18.842 |
| 15 | 5.316 | 6.720 | 5.672 | 15.695 | 17.098 | 20.806 |
| 16 | 5.965 | 8.690 | 6.957 | 18.207 | 20.933 | 23.669 |
| 17 | 7.908 | 11.900 | 10.343 | 21.908 | 25.901 | 28.907 |
| 18 | 11.149 | 16.200 | 14.555 | 26.491 | 31.542 | 34.820 |
| 19 | 13.921 | 19.700 | 18.148 | 30.166 | 35.945 | 39.538 |
| 20 | 15.569 | 21.700 | 20.280 | 32.265 | 38.396 | 42.227 |
| 21 | 17.397 | 24.000 | 22.642 | 34.543 | 41.147 | 45.141 |
| 22 | 21.739 | 29.400 | 28.244 | 39.777 | 47.438 | 51.825 |
| 23 | 29.976 | 39.000 | 38.847 | 49.318 | 58.342 | 63.989 |
| 24 | 40.968 | 51.000 | 52.958 | 61.546 | 71.579 | 79.560 |
| 25 | 55.508 | 66.300 | 71.582 | 77.233 | 88.024 | 99.517 |
| 26 | 74.598 | 84.000 | 95.984 | 97.360 | 106.762 | 125.113 |
| 27 | 99.515 | 105.000 | 127.785 | 123.195 | 128.680 | 157.959 |
| 28 | 131.886 | 131.886 | 126.602 | 156.363 | 156.363 | 155.315 |
| 29 | 173.786 | 173.785 | 238.505 | 198.941 | 198.941 | 285.089 |
| 30 | 234.946 | 234.946 | 200.632 | 258.905 | 258.905 | 219.048 |
| 31 | 166.956 | 166.955 | 188.882 | 177.050 | 177.050 | 201.176 |
| 32 | 226.779 | 226.779 | 240.137 | 235.744 | 235.744 | 251.487 |
| 33 | 382.746 | 382.746 | 410.987 | 394.376 | 394.376 | 427.349 |
| 34 | 852.713 | 852.713 | 776.741 | 874.451 | 874.451 | 797.536 |
| 35 | 189.613 | 189.613 | 193.059 | 192.723 | 192.723 | 200.154 |
| 36 | 186.505 | 186.515 | 208.933 | 192.983 | 192.983 | 222.100 |
| 37 | 968.372 | 968.372 | 1058.321 | 979.586 | 979.586 | 1071.782 |
| 38 | 9946.753 | 9946.753 | 9946.750 | 10037.175 | 10037.175 | 10037.172 |
| 39 | 6315.660 | 6315.650 | 6315.668 | 6335.918 | 6335.918 | 6335.926 |
| 40 | 1904.782 | 1904.782 | 1904.797 | 1908.483 | 1908.482 | 1908.493 |
| 41 | 1843.263 | 1843.263 | 1843.258 | 1845.402 | 1845.401 | 1845.397 |
| 42 | 9377.206 | 9377.205 | 5193.921 | 9380.588 | 9380.588 | 5196.625 |

## Table IV

### Eu-153 Capture and Total Infinitely Dilute Neutron Cross Sections

| Group No. | $\sigma_c$, barns | | | $\sigma_t$, barns | | |
|---|---|---|---|---|---|---|
| | Eu-A | Eu-D | Eu-H | Eu-A | Eu-D | Eu-H |
| 1 | .009 | .029 | .003 | 4.839 | 4.860 | 4.794 |
| 2 | .015 | .058 | .022 | 5.406 | 5.448 | 5.401 |
| 3 | .029 | .107 | .110 | 6.503 | 6.580 | 6.429 |
| 4 | .066 | .179 | .267 | 7.321 | 7.434 | 6.824 |
| 5 | .141 | .256 | .403 | 7.502 | 7.617 | 6.712 |
| 6 | .181 | .346 | .430 | 7.794 | 7.959 | 6.721 |
| 7 | .242 | .481 | .449 | 8.097 | 8.336 | 6.942 |
| 8 | .326 | .657 | .482 | 8.331 | 8.661 | 7.180 |
| 9 | .520 | .895 | .591 | 8.775 | 9.150 | 7.740 |
| 10 | .978 | 1.120 | .939 | 9.654 | 9.796 | 8.802 |
| 11 | 1.351 | 1.410 | 1.444 | 10.520 | 10.579 | 10.090 |
| 12 | 1.806 | 1.960 | 1.814 | 11.690 | 11.844 | 11.696 |
| 13 | 2.586 | 2.860 | 2.298 | 13.074 | 13.348 | 13.694 |
| 14 | 3.372 | 3.760 | 3.036 | 14.365 | 14.754 | 15.611 |
| 15 | 4.124 | 4.620 | 3.448 | 15.434 | 15.930 | 16.711 |
| 16 | 5.257 | 6.260 | 4.444 | 16.892 | 17.895 | 18.527 |
| 17 | 5.578 | 8.670 | 6.333 | 17.897 | 20.990 | 21.495 |
| 18 | 7.868 | 11.700 | 8.904 | 21.267 | 25.099 | 25.134 |
| 19 | 9.838 | 14.100 | 11.099 | 23.970 | 28.232 | 28.035 |
| 20 | 11.013 | 15.500 | 12.403 | 25.515 | 30.002 | 29.687 |
| 21 | 12.320 | 17.000 | 13.847 | 27.191 | 31.872 | 31.477 |
| 22 | 15.434 | 20.700 | 17.276 | 31.044 | 36.310 | 35.582 |
| 23 | 21.369 | 27.300 | 23.026 | 38.069 | 44.000 | 43.053 |
| 24 | 29.327 | 35.900 | 31.028 | 47.075 | 53.648 | 52.814 |
| 25 | 39.898 | 46.900 | 42.230 | 58.630 | 65.632 | 64.869 |
| 26 | 53.824 | 60.300 | 56.985 | 73.457 | 79.934 | 80.586 |
| 27 | 72.050 | 76.500 | 76.297 | 92.491 | 96.941 | 100.754 |
| 28 | 95.779 | 95.779 | 95.453 | 116.927 | 116.927 | 121.730 |
| 29 | 126.541 | 126.541 | 151.494 | 148.297 | 148.297 | 177.334 |
| 30 | 153.817 | 153.816 | 80.177 | 174.068 | 174.068 | 91.750 |
| 31 | 238.876 | 238.875 | 240.439 | 260.202 | 260.202 | 261.353 |
| 32 | 297.605 | 297.605 | 309.875 | 313.655 | 313.655 | 328.715 |
| 33 | 96.357 | 96.357 | 83.851 | 100.978 | 100.978 | 91.790 |
| 34 | 640.032 | 640.032 | 626.050 | 652.323 | 652.323 | 641.604 |
| 35 | 906.989 | 906.989 | 1023.501 | 919.703 | 919.703 | 1042.573 |
| 36 | 113.035 | 113.035 | 111.869 | 115.206 | 115.206 | 116.404 |
| 37 | 35.240 | 35.240 | 36.262 | 38.512 | 38.512 | 41.029 |
| 38 | 188.659 | 188.659 | 188.659 | 192.498 | 192.498 | 192.498 |
| 39 | 105.384 | 105.384 | 105.384 | 109.242 | 109.242 | 109.242 |
| 40 | 105.261 | 105.261 | 105.261 | 109.479 | 109.479 | 109.479 |
| 41 | 146.977 | 146.977 | 146.977 | 151.410 | 151.410 | 151.410 |
| 42 | 453.905 | 453.905 | 290.094 | 458.662 | 458.662 | 294.751 |

Table V

42-Group Energy and Lethargy Structure

| GROUP | LOWER ENERGY BOUNDARY[a] (ev) | LETHARGY INTERVAL |
|---|---|---|
| 1 | 6.065 + 6 | .5 |
| 2 | 3.679 + 6 | .5 |
| 3 | 2.231 + 6 | .5 |
| 4 | 1.353 + 6 | .5 |
| 5 | 8.208 + 5 | .5 |
| 6 | 4.979 + 5 | .5 |
| 7 | 3.877 + 5 | .25 |
| 8 | 3.020 + 5 | .25 |
| 9 | 1.832 + 5 | .5 |
| 10 | 1.111 + 5 | .5 |
| 11 | 6.738 + 4 | .5 |
| 12 | 4.087 + 4 | .5 |
| 13 | 2.554 + 4 | .47 |
| 14 | 1.989 + 4 | .25 |
| 15 | 1.503 + 4 | .28 |
| 16 | 9.119 + 3 | .5 |
| 17 | 5.531 + 3 | .5 |
| 18 | 3.355 + 3 | .5 |
| 19 | 2.840 + 3 | .167 |
| 20 | 2.404 + 3 | .167 |
| 21 | 2.035 + 3 | .167 |
| 22 | 1.234 + 3 | .5 |
| 23 | 7.485 + 2 | .5 |
| 24 | 4.540 + 2 | .5 |
| 25 | 2.754 + 2 | .5 |
| 26 | 1.670 + 2 | .5 |
| 27 | 1.013 + 2 | .5 |
| 28 | 6.144 + 1 | .5 |
| 29 | 3.727 + 1 | .5 |
| 30 | 2.260 + 1 | .5 |
| 31 | 1.371 + 1 | .5 |
| 32 | 8.315 + 0 | .5 |
| 33 | 5.043 + 0 | .5 |
| 34 | 3.059 + 0 | .5 |
| 35 | 1.855 + 0 | .5 |
| 36 | 1.125 + 0 | .5 |
| 37 | 6.826 - 1 | .5 |
| 38 | 4.140 - 1 | .5 |
| 39 | 2.511 - 1 | .5 |
| 40 | 1.523 - 1 | .5 |
| 41 | 9.237 - 2 | .5 |
| 42 | Thermal | .5 |

a Highest energy is 10 MeV.

dimensional model of the EMC was prepared to obtain the approximate neutron spectrum in the row 5 rod and row 7 rod locations. Table VI gives the dimensions, mesh spacing, and compositions used in the 1DX[17] code for this calculation. Cross sections for the removal of neutrons from each energy group due to elastic scattering were obtained for $^{151}Eu$, $^{153}Eu$, and $^{16}O$. The row 5 cross sections were obtained in 30 groups, the row 7 cross sections were in 42 groups.

Similar computations were done to obtain the down-scattering cross sections for $^{10}B$, $^{11}B$, and C.

4.1.6 Flux Depression in Absorber Platelets

In diffusion theory calculations, reaction rates are computed for each mesh interval from the product of the neutron flux and the macroscopic cross section in the mesh interval. Cross sections are input by zone. When strong absorbers are present in platelets smaller than the dimensions of a zone, the average flux actually seen by the absorber atoms may be less than the average flux in the zone due to local flux depressions caused by the strong absorber. This effect tends to make the computed absorber worth too large.

To determine the magnitude of the reactivity error, transport calculations were made using the DTF-IV[18] computer code and a one-dimensional model of the $Eu_2O_3$ compositions shown in Figure 2. Similar calculations were made for the $B_4C$ compositions. The results[19] showed that the calculated worths could be as much as 4.6% too high for the Eu #1 loading, but not more than 1.2% too high for the Eu #4 loading. The boron carbide platelets used for $B_4C$ loading #s 1-4 were a lower fraction of theoretical density than the europia platelets and consequently had lower worths and smaller flux depression effects, ranging from a maximum of 2.7% down to about 0.8%. Since the calculations were done in one-dimensional slab geometry they were intended to establish an upper limit to the reactivity error caused by the flux depression in the absorber platelets. However, additional studies have raised some doubts about the validity of the transport calculations. Due to these uncertainties, the

Table VI

Radial One-Dimensional Model of FTR-EMC

| Outer Radius cm | Number of Mesh Intervals | Zone Number | Material[a] |
|---|---|---|---|
| 6.319 | 4 | 1 | ID |
| 16.719 | 5 | 2 | 68% ID, 16% MT, 16% GP |
| 27.545 | 6 | 3 | 76% ID, 24% NA |
| 38.439 | 6 | 4 | 73% ID, 16% MT, 5.5% GP, 5.5% SP |
| 42.533 | 3 | 5 | OD |
| 45.200 | 4 | 8 | 50% CR, 50% NA |
| 49.356 | 3 | 5 | OD |
| 60.581 | 5 | 6 | OD |
| 65.294 | 3 | 7 | RR |
| 66.205 | 2 | 9 | PS |
| 89.145 | 7 | 7 | RR |
| 91.685 | 2 | 10 | NG |

a Material Notation:

| | | | |
|---|---|---|---|
| ID | Inner Driver | CR | Control Rod |
| OD | Outer Driver | PS | Peripheral Shim |
| RR | Radial Reflector | MT | Material Test |
| GP | General Purpose Loop | SP | Special Purpose Loop |
| NA | Sodium Channel | NG | Sodium Gap |

calculated control rod worths have not been adjusted to account for these spatial flux depressions. Further studies are planned to validate or correct the transport methods to account for this effect.

#### 4.1.7 EMC Cross Sections Other Than $Eu_2O_3$ and $B_4C$

The discussion of multigroup cross section preparation methods in this report has been concerned with the $Eu_2O_3$ and $B_4C$ cross sections. The preparation of 30-group and 42-group cross section sets for the EMC has been described in an earlier report[20]. The $Eu_2O_3$ and $B_4C$ cross sections were combined with the other EMC cross sections using the code, SORTXS, as indicated in Figure 6. The end result was one set of cross sections for the EMC in 30 groups containing $Eu_2O_3$ and $B_4C$ cross sections prepared for the row 5 location and another set in 42 groups with $Eu_2O_3$ and $B_4C$ cross sections prepared for row 7. To check the effect of 42 groups vs. 30 groups in the row 7 location, $Eu_2O_3$ cross sections were also prepared for row 7 in 30 groups. The results of this comparison were discussed in Section 4.1.3.

### 4.2 Calculational Model

#### 4.2.1 Geometry of 2-D X-Y Model

The computation of $k_{eff}$ for each reactor configuration assembled in the experiments was done with the two-dimensional diffusion theory code, 2DBS[21]. The computations were done in X-Y geometry because the experiment included only configurations with the abosrber rods either fully inserted or fully withdrawn. No configurations were assembled with partially inserted rods.

The model of the EMC used for the computations in this study is shown in Figure 7. The type of material in each zone of the figure is given in Table VII. The atom densities for Zones 4, 5, 6, 13 and 14 are given in Table VIII. Atom densities for all other numbered zones are given in Reference 1. The shaded zone in Figure 7 contained a combination of sodium gap and radial reflector, shield type 1 or shield type 2 composition. The zones labeled A, B, and C were the three locations

## Table VII

Compositions Used in Two-Dimensional X-Y Calculations

| Zone No. | Composition |
|---|---|
| 1 | Inner Driver |
| 2 | Outer Driver |
| 3 | Radial Reflector |
| 4 | Empty Matrix Tubes |
| 5 | Outer Driver Type A Partial Drawer with ZPR-9 Safety Rod Cavity |
| 6 | Outer Driver Type B Partial Drawer with ZPR-9 Safety Rod Cavity |
| 7 | Special Purpose Loop |
| 8 | General Purpose Loop |
| 9 | Material Test |
| 10 | Sodium Channel |
| 11 | Control Rod |
| 12 | Peripheral Shim Rod |
| 13 | Shield Type 1 |
| 14 | Shield Type 2 |

## Table VIII

EMC Atom Densities (Zones 4, 5, 6, 13 and 14)

| Isotope or Element | $10^{21}$ atoms/cm$^3$ | | | | |
|---|---|---|---|---|---|
| | Zone Numbers | | | | |
| | #4 | #5 | #6 | #13 | #14 |
| $^{238}$Pu | | 0.001 | 0.0005 | | |
| $^{239}$Pu | | 1.763 | 1.478 | | |
| $^{240}$Pu | | 0.233 | 0.174 | | |
| $^{241}$Pu | | 0.031 | 0.019 | | |
| $^{242}$Pu | | 0.004 | 0.002 | | |
| $^{235}$U | | 0.011 | 0.012 | | |
| $^{238}$U | | 5.008 | 5.117 | | |
| O | | 8.113 | 8.113 | | |
| Na | | 6.666 | 6.666 | 1.052 | 1.130 |
| Fe | 4.1516 | 13.719 | 13.443 | 53.265 | 46.344 |
| Cr | 1.1763 | 2.972 | 2.893 | 14.905 | 12.937 |
| Ni | 0.5096 | 1.376 | 1.340 | 6.188 | 5.335 |
| Mn | 0.0902 | 0.233 | 0.227 | 1.190 | 1.035 |
| Mo | 6.0059 | 0.461 | 0.440 | 0.082 | 0.072 |
| C | | 1.070 | 1.069 | 0.178 | 0.151 |
| Al | | | | 0.001 | 6.962 |

at which the $Eu_2O_3$ and $B_4C$ worths were measured. Zone A is SR-308, Zone B is CR-514 and Zone C is PSR-722.

The overall dimensions for the model were 204.64 cm in the horizontal direction and 193.58 cm in the vertical direction.

### 4.2.2 Mesh Spacing

A study was made to determine the effect of mesh spacing on the calculated worth of a control rod in the EMC (see Appendix C). The mesh spacing chosen for the europia worth experiment gave sixteen mesh points within a control rod. The primary advantage of this choice over one having four mesh intervals is the capability it affords to locate the absorber plates more accurately within the simulated control rod. Note, that in Figure 2, the europia platelets in compositions 1 and 2 are in the right half of the type A drawer.

Since the computer memory requirements and problem running time increase as the total number of mesh points in the problem increases, it was decided to have a lower mesh density over the remainder of the core. Thus, in Figure 7, in the horizontal direction from $X_0$ to $X_1$ and from $X_2$ to $X_3$ the mesh spacing was 5.531 cm. Between $X_1$ and $X_2$ the mesh spacing was 2.765 cm. Similarly, in the vertical direction the mesh spacing between $Y_1$ and $Y_2$ was 2.765 cm and was 5.531 cm over the remainder of the model. This mesh spacing gave 49 mesh intervals in the X direction and 41 in the Y direction for a total of 2,009 mesh intervals for the entire problem.

The zone labeled B in Figure 7, which is CR-514, was subdivided into three zones, as shown in Figure 8. Zone C of Figure 7 was also subdivided into three zones in the same manner as Zone B. Since only $B_4C$ #4 and $Eu_2O_3$ #4 compositions were measured in Zone A, this zone was not subdivided.

### 4.2.3 Axial Buckling

In a two-dimensional X-Y diffusion theory problem, the axial, or Z, direction is treated by assuming an axial buckling. In this study an

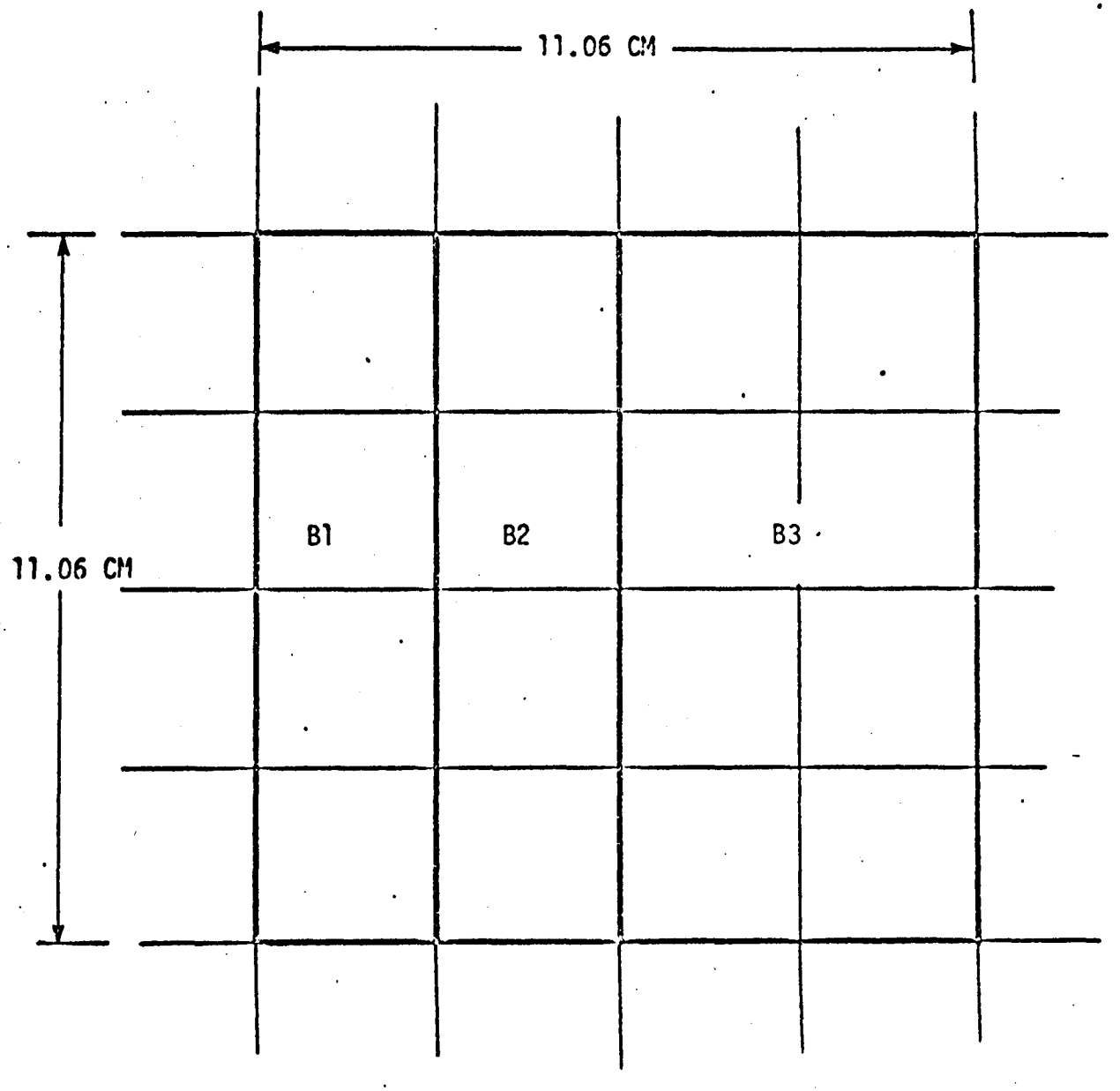


HEDL 7502-086.10

Figure 8. Zoning of CR-514 For The Europia Worth Experiment

energy independent buckling of 0.000565 $cm^{-2}$ was used in all computations for all regions of the reactor except the shield sector, Zones 13 and 14, and the empty matrix tubes, Zone 4. Zero axial buckling was used in these regions. The value of 0.000565 was obtained by determining the axial buckling in a 2-D X-Y problem that gave the same eigenvalue that was obtained in a 3-D X-Y-Z geometry diffusion theory calculation for the same assembly. This analysis[22] was done for the BOL-2 configuration which is very similar to BOL-REF-5. Another study was conducted to determine how much this effective axial buckling changes with changes in the number of safety, control or shim rods[23]. In the analysis of the europia worth experiment, the reactivities obtained from the eigenvalue calculations, using constant buckling, were adjusted to account for buckling changes caused by changes in the absorber rod configuration. These adjustments are discussed in Section 5.1.

#### 4.2.4 Convergence Criteria

The convergence criteria for the 2DBS eigenvalue calculations were set to insure that the maximum error in the computed rod worths would be less than the reported experimental uncertainties. The uncertainties in the computed values of $k_{eff}$ ranged from $0.6 \times 10^{-5}$ to $3.0 \times 10^{-5}$.

## 5. ANALYTICAL RESULTS

### 5.1 Buckling Adjustments

As pointed out in Section 4.2.3, the same value for the axial buckling of the FTR-EMC was used in all the two-dimensional calculations of $k_{eff}$ for this study. It has been shown[22] that it is necessary to use different values for the axial buckling in two-dimensional X-Y calculations for different core configurations in order to obtain the same eigenvalues that are computed in three-dimensional calculations for the same configurations. From a study of buckling sensitivity to changes in core configuration[23], estimates were obtained for the change in axial buckling due to the withdrawal of a safety rod or control rod or the removal of a peripheral shim.

For the complete removal of a safety or control rod the change in axial buckling can be treated as the sum of two parts: (1) the buckling change produced by withdrawing the rod from inserted to parked, and (2) the buckling change produced by removing the parked rod. The first part was obtained from Reference 23 and the second from the experimental data given in Section 3.3.1. Table IX gives the calculated change in buckling for the withdrawal of a 1% $\Delta k/k$ row 3 or row 5 rod or the removal of a 1% $\Delta k/k$ peripheral shim. It was assumed for the purposes of this study that the change in the axial buckling due to an absorber assembly was proportional to the worth of the assembly. Table IX also gives the calculated reactivity changes caused by the tabulated buckling changes. By adding to this the reactivity change due to the removal of the parked rods one obtains the total buckling induced reactivity change for the complete removal of an absorber assembly. A negative buckling change of $-10^{-6}$ $cm^{-2}$ causes a positive reactivity change of approximately 0.18% $\Delta k/k$. This says that in a two-dimensional X-Y diffusion theory calculation of rod worths, the use of a constant buckling results in an undercalculation of the rod worth. Therefore, the rod worths obtained from Eq. (1) should be multiplied by 1.0746 for the removal of a safety rod, by 1.0734 for the removal of a control rod, and by 1.0169 for the removal of a PSR.

## 5.2 $B_4C$ Worths

Table X gives the calculated worths of each $B_4C$ substitution relative to sodium channel composition. The results in the first column under "Reactivity Worth" were obtained from Eq. (1) using constant buckling. The values in the second column have been adjusted for buckling changes using the multipliers given in Section 5.1.

## 5.3 $Eu_2O_3$ Worths

As discussed in Section 4.1.3, calculations of the worths of europia compositions in the EMC were done with three different sets of cross section data: Eu-A, Eu-D, and Eu-H. The calculated worths of each europia composition with all three sets of cross section data are given in Table XI. Part A of Table XI gives the results obtained with constant buckling and Part B gives the results adjusted for buckling changes.

## Table IX

## Effect of Rod Removal on Axial Buckling and Buckling Induced Reactivity Change

| Absorber Rod Type | Buckling Change For Withdrawal of a 1% Δk/k Absorber Rod $10^{-6}$ cm$^{-2}$/1% Δk/k | Buckling Induced Reactivity Change For a 1% Δk/k Absorber Rod % Δk/k/% Δk/k | Reactivity Change Due to Removal of Parked Rods % Δk/k/% Δk/k | Total Buckling Induced Reactivity Change For a 1% Δk/k Absorber Rod % Δk/k/% Δk/k |
|---|---|---|---|---|
| Row 3 SR | -2.11 ± 0.17 | +0.0379 ± .0030 | +0.0367 ± .0022 | +0.0746 ± .0037 |
| Row 5 CR | -1.92 ± 0.04 | +0.0345 ± .0009 | +0.0389 ± .0033 | +0.0734 ± .0034 |
| Row 7 PSR | -0.94 ± 0.38 | +0.0169 ± .0069 | - | +0.0169 ± .0069 |

## Table X

## Calculated Worths of $B_4C$

| Location | $B_4C$ Composition | Reactivity Worth, % Δk/k | |
|---|---|---|---|
| | | Constant Buckling | With Buckling Adjustment |
| PSR-722 | 1 | -0.0457 ± .0031 | -0.0465 ± .0032 |
| PSR-722 | 2 | -0.0655 ± .0031 | -0.0666 ± .0032 |
| PSR-722 | 3 | -0.0941 ± .0031 | -0.0957 ± .0032 |
| PSR-722 | 4 | -0.1332 ± .0031 | -0.1354 ± .0033 |
| CR-514 | 1 | -0.1908 ± .0021 | -0.2048 ± .0024 |
| CR-514 | 2 | -0.3426 ± .0021 | -0.3677 ± .0026 |
| CR-514 | 3 | -0.6066 ± .0021 | -0.6511 ± .0031 |
| CR-514 | 4 | -1.0015 ± .0021 | -1.0750 ± .0041 |
| CR-514 | a | -1.3285 ± .0042 | -1.4260 ± .0064 |
| SR-308 | 4 | -1.4124 ± .0056 | -1.5178 ± .0079 |

a EMC $B_4C$ control rod composition (Ref. 8).

Table XI

Calculated Worths of $Eu_2O_3$

A. Constant Buckling

| Location | $Eu_2O_3$ Composition | Reactivity Worth, % Δk/k Eu-A[a] | Eu-D[b] | Eu-H[c] |
|---|---|---|---|---|
| PSR-722 | 1 | -0.0577 ± .0006 | -0.0667 ± .0031 | -0.0632 ± .0009 |
| " | 2 | -0.0757 ± .0009 | -0.0882 ± .0031 | -0.0818 ± .0009 |
| " | 3 | -0.1029 ± .0009 | -0.1235 ± .0031 | -0.1118 ± .0009 |
| " | 4 | -0.1363 ± .0009 | -0.1627 ± .0031 | -0.1467 ± .0009 |
| CR-514 | 1 | -0.2466 ± .0021 | -0.3136 ± .0021 | -0.2764 ± .0021 |
| " | 2 | -0.4074 ± .0021 | -0.5105 ± .0021 | -0.4470 ± .0021 |
| " | 3 | -0.6918 ± .0021 | -0.8532 ± .0021 | -0.7462 ± .0021 |
| " | 4 | -1.0664 ± .0021 | -1.2840 ± .0021 | -1.1346 ± .0021 |
| SR-308 | 4 | -1.5058 ± .0021 | -1.8194 ± .0042 | -1.5958 ± .0021 |

B. With Buckling Adjustment

| Location | $Eu_2O_3$ Composition | Reactivity Worth, % Δk/k Eu-A[a] | Eu-D[b] | Eu-H[c] |
|---|---|---|---|---|
| PSR-722 | 1 | -0.0587 ± .0008 | -0.0678 ± .0032 | -0.0643 ± .0010 |
| " | 2 | -0.0769 ± .0010 | -0.0897 ± .0032 | -0.0832 ± .0010 |
| " | 3 | -0.1046 ± .0011 | -0.1256 ± .0033 | -0.1137 ± .0012 |
| " | 4 | -0.1386 ± .0013 | -0.1654 ± .0033 | -0.1492 ± .0013 |
| CR-514 | 1 | -0.2647 ± .0024 | -0.3366 ± .0025 | -0.2967 ± .0024 |
| " | 2 | -0.4373 ± .0027 | -0.5480 ± .0029 | -0.4798 ± .0027 |
| " | 3 | -0.7426 ± .0034 | -0.9158 ± .0038 | -0.8010 ± .0036 |
| " | 4 | -1.1447 ± .0043 | -1.3782 ± .0049 | -1.2179 ± .0046 |
| SR-308 | 4 | -1.6181 ± .0059 | -1.9551 ± .0080 | -1.7148 ± .0062 |

a Eu-151 and Eu-153 cross sections from ENDF/B, Version 3.

b Eu-151 and Eu-153 cross sections evaluated by Schadel and Schenter (Ref. 11).

c Eu-151 and Eu-153 cross sections from ENDF/B, Version 4.

## 6. COMPARISON OF CALCULATED AND MEASURED RESULTS

Using the calculated worths with buckling corrections from Tables X and XI and the measured worths from Table II, ratios of calculated to experimental results were obtained and are shown in Table XII. The percent deviation from a C/E of 1.0 was obtained, as follows:

$$\% \text{ deviation} = (C/E - 1.0) \times 100.$$

These values are plotted as a function of volume fraction in Figure 9 for the PSR-722 location and in Figure 10 for the CR-514 location.

## 7. CONCLUSIONS

1. In small quantities, $Eu_2O_3$ has a higher worth than $B_4C$ on an equal volume basis, assuming the same percentage of theoretical density, at the CR-514 and PSR-722 locations.
2. As the volume fraction increases, $B_4C$ becomes more reactive than $Eu_2O_3$. This is true for both the CR and PSR locations. This indicates that self-shielding effects are greater for $Eu_2O_3$ than for $B_4C$.
3. The volume fraction at which the $B_4C$ worth becomes greater than the $Eu_2O_3$ worth is about 0.22 at the CR-514 location. This corresponds to a $B_4C$ mass of about 6.2 kg or a $^{10}B$ mass of about 880 grams.
4. At a volume fraction corresponding to the amount of $B_4C$ in an FTR control rod, a $B_4C$ rod at the CR-514 location is worth about 3 to 4% more than a $Eu_2O_3$ rod on an equal volume basis.
5. The experimental accuracy at the PSR-722 location was not as good as at the CR-514 location; however, the data for the PSR-722 location are consistent with conclusions 3 and 4 above.
6. Using the analytical methods described in this report, the calculated worth of $B_4C$ is a few percent higher than the measured worth in the CR-514 and SR-308 locations and a few percent lower than the measured worth in the PSR-722 location.

## Table XII

## Ratios of Calculated (C) to Experimental (E) Results

| Control Rod Location | Composition Number | C/E[a] | | | |
|---|---|---|---|---|---|
| | | $B_4C$ | Eu-A | Eu-D | Eu-H |
| PSR-722 | 1 | 0.963 ± .092 | 0.032 ± .049 | 1.076 ± .075 | 1.021 ± .054 |
| " | 2 | 0.928 ± .061 | 0.863 ± .036 | 1.007 ± .051 | 0.934 ± .035 |
| " | 3 | 0.934 ± .043 | 0.886 ± .026 | 1.064 ± .040 | 0.963 ± .027 |
| " | 4 | 0.916 ± .030 | 0.840 ± .018 | 0.998 ± .021 | 0.900 ± .020 |
| CR-514 | 1 | 1.039 ± .021 | 0.956 ± .014 | 1.216 ± .017 | 1.072 ± .015 |
| " | 2 | 1.043 ± .012 | 0.960 ± .009 | 1.203 ± .011 | 1.053 ± .008 |
| " | 3 | 1.078 ± .010 | 1.012 ± .008 | 1.248 ± .010 | 1.091 ± .009 |
| " | 4 | 1.102 ± .006 | 1.027 ± .009 | 1.236 ± .010 | 1.092 ± .009 |
| " | b | 1.102 ± .015 | - | - | - |
| SR-308 | 4 | 1.066 ± .010 | 0.997 ± .010 | 1.204 ± .013 | 1.056 ± .011 |

a Calculated worths include buckling adjustments.

b EMC $B_4C$ control rod composition (Ref. 8).

7. At a volume fraction corresponding to the amount of $B_4C$ in an FTR control rod, the C/E for $B_4C$ is 1.102 ± .015 at the CR-514 location.

8. An extrapolation of the $B_4C$ results at the PSR-722 location to a volume fraction corresponding to the amount of $B_4C$ in an FTR PSR cannot be done very accurately; however, a C/E of 0.90 ± .09 appears to be a reasonable estimate.

9. The EU-A cross sections give C/Es consistently lower than those for $B_4C$, the Eu-D cross sections give C/Es consistently higher than those for $B_4C$, and the Eu-H cross sections give results very similar to those for $B_4C$ at all three locations. On this basis it appears that the ENDF/B version 4 evaluations for $^{151}Eu$ and $^{153}Eu$ are preferable to the other two evaluations considered in this study.

10. Using the Eu-H cross sections and extrapolating to an FTR-type volume fraction, the C/E for the worth of a europia rod is 1.093 ± .015 at the CR-514 location and 0.89 ± .03 at the PSR-722 location.

## 8. APPLICATIONS AND RECOMMENDATIONS

The results obtained in this study can be used to adjust calculated worths of absorber rods in the FTR. For this procedure to be most effective the FTR calculations should utilize the same methods used for the EMC calculations as much as possible. However, there are differences between the EMC and the FTR that require some differences in calculational methods. The effects of some of these differences will be discussed below.

### 8.1 Heterogeneity Effects

The europia that was fabricated for use in the ANL zero power reactors (ZPR-6, -9, and ZPPR) was in the form of wafers with dimensions 0.200 in. x 1.955 in. x 5.700 in. These wafers were sealed in stainless steel cans with nominal outside dimensions 0.25 in. x 2.00 in. x 6.00 in. For the EMC these cans were then loaded into the ZPR-9 matrix, as indicated in Figures 2 and 3 with a total axial length of 36 inches.

For the FTR the europia will be fabricated into cylindrical pellets 0.379 in. in diameter and loaded into a stainless steel tube to make a

rod of europia 36 in. long. Sixty-one of these rods will be used in each hexagonal FTR europia absorber assembly.

Because of these geometric differences and the fact that $^{151}Eu$ and $^{153}Eu$ are resonant materials, the treatment of resonance and spatial self-shielding effects should be considered.

Europium resonance self-shielding was discussed in Section 4.1.4. For the EMC it was determined that a homogeneous resonance self-shielding treatment was adequate for the platelet geometries used in the experiment. In an FTR europia assembly the europia will be more homogeneously distributed than in the EMC. On this basis, homogeneous resonance self-shielding would also appear to be adequate for the FTR calculations of europia worth.

The spatial self-shielding effect was discussed in Section 4.1.6. This effect should be smaller in the FTR due to the more homogeneous distribution of the absorber material in the control rods. Since it was not accounted for in the EMC calculations and may be of different magnitude in the FTR, the bias factors cannot eliminate this effect as a possible source of error in FTR rod worth calculations. It is recommended, therefore, that future studies be made to determine if this effect is significant, and, if so, to determine the best method to account for it in rod worth calculations.

## 8.2 Mesh Spacing

Figure C-1 in Appendix C shows the effect of mesh spacing on calculated rod worths. The C/Es given in Section 6 of this report were obtained with sixteen mesh points per control rod. Since the FTR has hexagonal subassemblies, most rod worth calculations are done with six triangular mesh intervals per control rod.

Figure C-1 can be used to make bias factor adjustments for different mesh spacings (see Appendix C)

The adjusted bias factors for $B_4C$ and $Eu_2O_3$ worths at the CR-514 location in a two-dimensional calculation with six mesh triangles per subassembly are 1.037 ± .015 and 1.067 ± .015, respectively. For the SR-308 location the adjusted bias factors are 1.051 ± .015 for $B_4C$ and 1.031 ± .015 for $Eu_2O_3$.

## 8.3 C/E For FTR Rod Worths

In the preceding section (8.2) C/E bias factors were given for the worth of $B_4C$ and $Eu_2O_3$ control rod compositions relative to sodium channel composition in the CR-514 and SR-308 locations. These bias factors were based on the complete removal of the absorber material rather than withdrawing a simulated rod from the inserted condition to the parked condition. Both types of absorber rod manipulations will occur in the FTR, and therefore, bias factors are needed to adjust calculated rod worths for both cases.

In a previous study[8] of control rod interaction effects, C/Es were obtained for $B_4C$ control rod composition at four locations in the EMC. The C/Es were obtained for the withdrawal of the rods from inserted to parked using four mesh points per subassembly and constant buckling. The average C/E bias factor was 1.017. If the calculations are adjusted, using Figure C-1, to their expected values with six mesh intervals per subassembly, the average C/E becomes 1.026. If buckling adjustments are applied to the calculations (see Appendix D) the average C/E bias factor becomes 1.062 with a range of values from 1.008 to 1.116. The study showed that bias factors are spatially dependent, with differences within row 5 as large as differences between row 3 and row 5. With core conditions similar to those in the europia worth experiment, the C/E values from the rod interaction study at the CR-514 and SR-308 locations are 1.087 ± .016 and 1.059 ± .011, respectively (see Table D-I). These results are in good agreement with the values given in Section 8.2 for $B_4C$. This indicates that the C/E bias is the same for computing the worth of a rod removal or a rod withdrawal if the appropriate buckling adjustments are made.

The analysis of the europia experiments described in this report provides the only available information on C/E factors for europia rod worths. Based on the results given in Section 8.2, the C/E for in-core europia rods in the FTR using ENDF/B version 4 cross sections is about 2% less than the C/E for boron carbide rods.

The recommended C/E bias factors to apply to calculations of individual FTR safety rod (row 3) and control rod (row 5) worths are given in Table XIII.

Table XIII

Bias Factors For FTR Rod Worth Calculations

| Type of Rod | Recommended C/E Bias Factor[a] | | | |
|---|---|---|---|---|
| | For Rod Withdrawal | | For Rod Removal | |
| | With Constant Buckling | With Buckling Adjustment | With Constant Buckling | With Buckling Adjustment |
| $B_4C$ | 1.03 | 1.06 | 0.99 | 1.06 |
| $Eu_2O_3$ | 1.01 | 1.04 | 0.97 | 1.04 |

a EMC bias factors were spatial dependent. Individual rod worths may differ by ± 5% from calculated worths adjusted with these factors.

The C/E values are 4% lower for rod removal than for rod withdrawal with constant buckling because the experimental worth is 4% higher and the calculated worth is the same.

The bias factors in Table XIII are based on the following assumptions:

1. two-dimensional diffusion theory,
2. six triangular mesh intervals per subassembly,
3. 30 energy groups from FTR Set 300,
4. ENDF/B, version 4 europium cross sections,
5. calculated rod worths with constant buckling are increased by a factor of 1.074 for rod removal and by 1.035 for rod withdrawal.

The C/E of 1.03 for rod withdrawal with constant buckling is in agreement with results reported by Westinghouse Advanced Reactors Division (ARD) in the final design support document for FFTF control rods.

It should be noted, that the bias factors given in Table XIII are average values and that individual rod worths may differ by ± 5% from the calculated worths adjusted with these factors.

For the computation of peripheral shim worths in the FTR, bias factors have been obtained by combining the results of this study with those obtained in the analysis of control rod interaction effects[8].

There appears to be no advantage to be gained from the use of buckling adjustments in computing the worths of peripheral shims. The recommended C/E bias factors with constant buckling are 0.95 for $B_4C$ or $Eu_2O_3$ shims using ENDF/B version 4 cross sections for europium. Individual rod worths may differ by ± 7% from the calculated worths adjusted with these factors.

## 9. REFERENCES


1) J.W. Daughtry, C.D. Swanson, A.B. Long, R.B. Pond and G.K. Rusch, "ZPR-9 Assembly 27: The Fast Test Reactor Engineering Mockup Critical (FTR-EMC)," Applied Physics Division Annual Report for July 1, 1970 to June 30, 1971, ANL-7910, Pg. 32-39, January 1972.

2) A. Travelli, A.J. Ulrich and J.C. Beitel, "Planning and Analysis in Support of the Fast Flux Test Facility (FFTF) Critical Experiments in ZPR-9," Applied Physics Division Annual Report for July 1, 1970 to June 30, 1971, ANL-7910, Pg. 56-61, January 1972.

3) R.A. Bennett and P.L. Hofmann, "Rationale and Plans for the FTR Critical Experiments Program," BNWL-490, Battelle Northwest, Richland, WA, June 1967.

4) R.B. Pond, W.R. Robinson and R.J. Armani, "Europia Worth Measurements in the FTR-EMC," Reactor Development Program Progress Report for January 1974, ANL-RDP-24, Pg. 6.4-6.12, February 1974.

5) S.K. Bhattacharyya, R.B. Pond, D.M. Smith and W.R. Robinson, "Measurement of Control Rod Worths in the High-$^{240}$Pu Fueled Sector," ZPR-TM-184, Table VII, Argonne National Laboratory, December 1974.

6) A.C. Larson and D.T. Cramer, "Reexamination of the Crystal Structure of '$B_4C$'," Acta Crystallogr. A (Denmark), Vol. A28, Pt. 4, Suppl., Pg. S53, 1972.

8) J.W. Daughtry, J.F. Meyer and A. Travelli, "Control Rod Interaction Effects in Sodium Cooled Fast Reactors," Proceedings of the Atlanta ANS Topical Meeting on 'Advanced Reactors: Physics, Design and Economics'," to be published.

9) A.E. Pasto, "Europium Oxide as a Potential LMFBR Control Material," ORNL-TM-4226, Pg. 12, September 1973.

10) ENDF/B Version 3 Cross Section and Nuclear Data Files. Available from NNCSC, Brookhaven National Laboratory, Brookhaven, NY.

11) H.M. Schadel, III and R.E. Schenter, "Europium Cross Section Calculations," HEDL Quarterly Technical Report, HEDL-TME 73-5, Vol. 2, Pg. A-4, October 1973.

12) ENDF/B Version 4 Cross Section and Nuclear Data Files. Available from NNCSC, Brookhaven National Laboratory, Brookhaven, NY.

13) R.E. Schenter, J.L. Baker and R.B. Kidman, "ETOX, A Code to Calculate Group Constants for Nuclear Reactor Calculations," BNWL-1002, Battelle Northwest Laboratory, Richland, WA, May 1969.

14) I.I. Bondarenko et al, Group Constants for Nuclear Reactor Calculations, Consultants Bureau, New York, 1964.

15) R.E. Schenter, R.B. Kidman and J.V. Nelson, "FTR Set 300, Multigroup Cross Sections for FTR Design," HEDL-TME 71-153, Hanford Engineering Development Laboratory, Richland, WA, October 1971.

16) R.B. Kidman and R.E. Schenter, "FTR Set 300-S, Multigroup Cross Sections for FTR Shielding Calculations," HEDL-TME 71-184, Hanford Engineering Development Laboratory, Richland, WA, December 1971.

17) R.W. Hardie and W.W. Little, Jr., "1DX, A One-Dimensional Diffusion Theory Code for Generating Effective Nuclear Cross Sections," BNWL-954, Battelle Northwest Laboratory, Richland, WA, March 1969.

18) K.D. Lathrop, "DTF-IV, A Fortran-IV Program for Solving the Multigroup Transport Equation with Anisotropic Scattering, LA-3373, Los Alamos Scientific Laboratory, Los Alamos, NM, November 1965.

19) J.W. Daughtry, "Analysis of Europia Worth Measurements in the FTR Engineering Mockup," HEDL Quarterly Technical Progress Report for July-September 1974, HEDL-TME 74-3, Vol. 3, Pg. A-3 - A-8, Hanford Engineering Development Laboratory, Richland, WA, October 1974.

20) R.M. Fleischman, "Evaluation of the Modified Source Multiplication Technique for Subcritical Reactivity Assessments in FTR," HEDL-TME 74-53, Appendix A, Hanford Engineering Development Laboratory, Richland, WA, October 1974.

21) D.R. Marr, "A User's Manual for 2DBS, A Diffusion Theory Shielding Code," BNWL-1291, Battelle Northwest Laboratory, Richland, WA, February 1970.

22) R.M. Fleischman and J.V. Nelson, "Three-Dimensional Neutronics Calculations for the Fast Test Reactor (FTR) and the FTR Engineering Mockup Critical Assembly (EMC)," HEDL-TME 72-42, Pg. 14, Hanford Engineering Development Laboratory, Richland, WA, April 1972.

23) J.V. Nelson and Q.L. Baird, "Three-Dimensional Buckling Calculations," HEDL Quarterly Technical Progress Report for April-June 1974, HEDL-TME 74-2, Vol. 3, Pg. 1-1 - 1-3, Hanford Engineering Development Laboratory, Richland, WA, July 1974.

# APPENDIX A

## REACTIVITY LOSS DUE TO $^{241}$PU DECAY

The FTR engineering mockup critical experiments were conducted in the ZPR-9 facility at Argonne National Laboratory from February 1971 through May 1974. In a time period of this magnitude, the radioactive decay of $^{241}$Pu had an observable effect on the reactivity of the assembly. Pu-241 decays with a half life of 14.8 ± .2 years[1], primarily by β decay[2] to $^{241}$Am. A determination of the reactivity change due to the decay of $^{241}$Pu was made by measuring the reactivity of the same reactor configuration several times over a period of approximately eleven months. Table A-I gives the dates of the measurements and the reactivities of the assembly[3]. Over a time span of one year, exponential decay with a 14.8-year half life can be adequately approximated by a straight line. A least squares fit of the reactivity data to a straight line gave a rate of reactivity loss of 0.205 ±.0.022 inhours per day.

A calculated value for the reactivity worth of $^{241}$Pu was obtained from a pair of two-dimensional X-Y calculations for the BOL-REF-5 configuration of the FTR-EMC. The only differences between the two calculations were the concentrations of $^{241}$Pu in the inner and outer driver zones. The computed rate of reactivity loss was 0.159 ± 0.005 inhours per day. The calculation was done in 30 groups using FTR Set 300[4]. Any effect due to the increase in the amount of $^{241}$Am was ignored.

The experimentally determined value of 0.205 ± 0.022 inhours per day should be used to adjust experimental data when it is necessary to compare the reactivities of the assembly at different times during the experimental program.

Table A-I

Reactivity of FTR-EMC
Configuration BOL-REF-5S

| Date | Reactivity (Inhours) |
|---|---|
| 8-14-73 | 93.9 ± 2.4 |
| 10-15-73 | 77.9 ± 2.4 |
| 11-15-73 | 79.0 ± 2.5 |
| 12-17-73 | 73.5 ± 2.4 |
| 3-12-74 | 59.7 ± 2.4 |
| 6-26-74 | 25.2 ± 2.4 |

References:


1) ENDF/B-IV Cross Section and Nuclear Data Files. Available from NNCSC, Brookhaven National Laboratory, Brookhaven, New York.

2) C.M. Lederer, J.M. Hollander and J. Perlman, "Table of Isotopes," J. Wiley & Sons, New York, 6th Edition, Pg. 435, 1967.

4) R.E. Schenter, R.B. Kidman and J.V. Nelson, "FTR Set 300, Multigroup Cross Sections for FTR Design," HEDL-TME 71-153, October 1971.

## APPENDIX B

## EUROPIUM RESONANCE SELF-SHIELDING

A study was made to determine how to account for resonance self-shielding effects in the four europium compositions used in the europia worth experiment. The methods employed by the ETOX-1DX system[1,2] to obtain shielded cross sections are described in Reference 3. Effective cross sections, $\bar{\sigma}$, are obtained from the product:

$$\bar{\sigma} = f\langle\sigma\rangle \qquad \text{(B-1)}$$

where $\langle\sigma\rangle$ represents the infinitely dilute cross section (i.e., no resonance self-shielding) and 'f' is the shielding factor (or f-factor). The ETOX code provides the infinitely dilute cross sections in a specified group structure and tables of shielding factors. For a given isotope, shielding factors are determined for each energy group and cross section type (fission, capture, elastic scattering and total). The f-factors are a function of the temperature and the quantity, $\sigma_0$, that depends on the composition, environment, and geometry of the material.

Europium cross sections were prepared for a temperature of 300°K. All experimental results were reported for a reactor temperature of 25°C, which is approximately 298°K. The difference between 298°K and 300°K was not significant in this study.

The 1DX code has been modified[4] to provide a more accurate resonance self-shielding treatment for the platelet critical experiments performed in the ZPRs. In the modified 1DX, $\sigma_0$ is defined by:

$$\sigma_{0,k} = \frac{\sum_{\ell} t^{(p)}}{N_k} + \frac{(1-C)\,A}{\bar{\ell}(1+(A-1)C)N_k} \qquad \text{(B-2)}$$

where,

$\sigma_{o,k}$ = effective total cross section per atom of isotope k,

$\Sigma_t^{(p)}$ = macroscopic total cross section in plate excluding isotope k,

$N_k$ = atom density of isotope k in plate,

A = Levine parameter[5],

C = Dancoff factor[6],

$\bar{\ell}$ = 4V/S = mean chord length of plate,

V = volume of plate,

S = surface area of plate.

The resonance self-shielding of a material is accounted for in this calculational scheme by reducing the infinitely dilute cross sections by the shielding factors, f. Once the temperature is specified, the f-factors are a function only of $\sigma_{o,k}$. In those energy groups of a material having resonances, as $\sigma_{o,k}$ decreases, the f-factors decrease which means an increase in the resonance self-shielding and a decrease in the effective cross section.

The first term in the expression for $\sigma_{o,k}$ (Eq. B-2) represents the macroscopic total cross section of all materials except isotope k in the platelet per atom of isotope k. This would be the value of $\sigma_{o,k}$ for an infinite medium of platelet material. The second term of Eq. (B-2) increases the value of $\sigma_{o,k}$ (decreases the resonance self-shielding) for the case of an isolated lump or a heterogeneous array.

For a homogeneous medium, C=1, and $\sigma_{o,k} = \frac{\Sigma_t}{N_k}$. (B-3)

For an isolated lump of material, C=0, and

$$\sigma_{o,k} = \frac{\Sigma_t^{(lump)}}{N_k} + \frac{A}{\bar{\ell} N_k} \quad . \tag{B-4}$$

The isolated lump approximation was used in preparing cross sections for Eu#1 and Eu#2 with an A of 1.25 and an $\bar{\ell}$ of 0.9696 cm and 2.0637 cm, respectively. These cross sections were used in computing the worths of the Eu#1 and Eu#2 compositions in this analysis.

For Eu#3 the resonance self-shielding is expected to be greater than for Eu#1 due to the presence of the other plates. Similarly, the resonance self-shielding should be greater for Eu#4 than for Eu#2. Eq. (B-2) can be used to obtain values of $\sigma_o$ for an infinite heterogeneous medium of absorber plates; however, for arrays such as Eu#3 and Eu#4, which consist of a few plates of finite size, Eq. (B-2) cannot be applied directly. It is obvious, though, that the $\sigma_o$ values for Eu#3 will lie between those for the Eu#1 isolated lump case and those for an infinite medium of plates in an array similar to that of Eu#3. Cross sections were prepared for the infinite heterogeneous medium of europia platelets assuming a Dancoff factor, C, given by

$$C = 2E_3\left(\Sigma_t^{(d)} \frac{\bar{\ell} V_d}{2V_p}\right) \tag{B-5}$$

where $\Sigma_t^{(d)}$ is the total cross section of the diluent material within a control rod and $V_d/V_p = t_d/t_p$. The ratio of diluent volume to europia plate volume is assumed to be equal to the ratio of their thicknesses. In this case, $\bar{\ell} = 2\ t_p$.

The reactivity worth of the Eu#3 composition was computed with these cross sections and with the Eu#1 isolated lump cross sections. The difference between the computed worths was negligible. A similar comparison was made for the Eu#4 composition with the same results. Further studies showed that homogeneously resonance self-shielded cross sections based on the Eu#4 atom densities could be used for all calculations without significant error.

This does not mean that resonance self-shielding is unimportant in this case; e.g., infinitely dilute cross sections give europia rod worths that are significantly higher than those obtained with cross sections prepared for any of the cases discussed above.

References:


1) R.E. Schenter, J.L. Baker, and R.B. Kidman, "ETOX, A Code to Calculate Group Constants for Nuclear Reactor Calculations," BNWL-1002, Battelle Northwest Laboratory, 1969.

2) R.W. Hardie and W.W. Little, Jr., "1DX, A One-Dimensional Diffusion Code for Generating Effective Nuclear Cross Sections," BNWL-954, Battelle Northwest Laboratory, 1959.

3) R.B. Kidman, R.E. Schenter, R.W. Hardie, and W.W. Little, "The Shielding Factor Method of Generating Multigroup Cross Sections for Fast Reactor Analysis," Nucl. Sci. Eng., Vol. 48, Pg. 189-201, 1972.

4) R.A. Harris and R.A. Bennett, "Improved Resonance Self-Shielding in 1DX," HEDL Quarterly Technical Report for April, May, June 1973, HEDL-TME 73-4, Vol. 2, Pg. 1-1, August 1973.

5) M.M. Levine, "Resonance Integral Calculations for $^{238}U$ Lattices," Nucl. Sci. Eng., Vol. 16, Pg. 271, 1963.

6) J.R. Lamarsh, "Introduction to Nuclear Reactor Theory," Addison-Wesley Publishing Co., Inc., Reading, MA, pg. 400, 1966.

## APPENDIX C

### EFFECT OF MESH SIZE ON COMPUTED ROD WORTHS

A series of calculations was performed to determine the effect of mesh size on the computed worth of simulated control rods in the FTR-EMC using two-dimensional diffusion theory. The analysis was done for both $B_4C$ and $Eu_2O_3$ control rods at the CR-514 location. The EMC control rods had a square cross sectional area 11.0617 cm on a side. The two-dimensional calculations were done in X-Y geometry with the 2DBS code[1]. The rod worth calculations were done with three different mesh spacings: 5.531 cm, 2.765 cm and 1.383 cm giving 4, 16, and 64 mesh intervals in the control rod. The mesh spacing that was used in the rod was also used outside the rod for a distance of 5.531 cm in both X and Y directions. The worths of two $B_4C$ and two $Eu_2O_3$ compositions were computed. The results are shown in Figure C-1.

In every case the rod worth increases in a nearly linear manner with decreasing mesh spacing. The higher worth rods are more sensitive to mesh size than the lower worth rods, and the europia rods are more sensitive to mesh spacing than the boron carbide rods.

Since the calculated worth of a control rod depends on the mesh size used in the calculation, the C/E bias factors for control rod worth will also depend on the mesh size. The cross sectional area of a simulated control rod in the FTR-EMC was only slightly (about 3%) less than that of a hexagonal FTR rod. The most commonly used model for neutronics calculations of FTR core characteristics employs six triangular mesh intervals per subassembly. The cross sectional area of each triangular mesh interval is about 21 $cm^2$. A mesh spacing of 4.58 cm in X-Y geometry would give the same cross sectional area. This mesh spacing is indicated on the graph in Figure C-1.

For application to the FTR, bias factors should be based on calculated rod worths that have been adjusted to this 4.58 cm mesh spacing. Table C-I shows how the mesh adjustment was determined for an in-core $B_4C$ rod. The value obtained was 0.986. This means that the calculated worths of in-core $B_4C$ control rods obtained with 16 mesh intervals per subassembly and the corresponding C/E bias factors should be reduced by 1.4% when the results

are to be used to correct FTR calculations using six triangles per subassembly. With this adjustment the bias factor of 1.102 ± .015 for $B_4C$ at the CR-514 location given in Conclusion No. 7 of Section 7 becomes: (1.102 ± .015) x 0.986 = 1.087 ± .015.

Table C-I

Mesh Spacing Adjustment for An In-Core $B_4C$ Rod

| Control Rod Identification | $^{10}B$ Content, grams | Mesh[a] Adjustment | Source |
|---|---|---|---|
| EMC-$B_4C$ | 1324 | 0.984 | From Fig. C-1 |
| $B_4C$ #4 | 862 | 0.990 | From Fig. C-1 |
| FTR-$B_4C$ (nominal) | 1206 | 0.986 | Interpolated[b] |

a Ratio of calculated worth with six mesh intervals to worth with 16 mesh intervals.

b Assuming linear variation of mesh adjustment with $^{10}B$ content.

The amount of $Eu_2O_3$ in the first FTR rods of this type is to be chosen to give the same worth as an FTR-$B_4C$ control rod. The nominal $B_4C$ loading in an FTR rod is 1206 grams which corresponds to a volume fraction of 0.303 based on maximum theoretical density. Using the curves in Figure 5, a $Eu_2O_3$ volume fraction of 0.324 will give the same worth as the nominal FTR-$B_4C$ loading. Table C-II shows that the mesh adjustment for an FTR-$Eu_2O_3$ rod should be 0.976 or a 2.4% reduction in the worths obtained with 16 mesh points per subassembly. When this adjustment is applied to the C/E for the CR-514 location given in Conclusion No. 10 of Section 7, this value becomes (1.093 ± .015) x 0.976 = 1.067 ± .015.

Table C-II

Mesh Spacing Adjustment For An In-Core $Eu_2O_3$ Rod

| Control Rod Identification | Volume[a] Fraction | Mesh[b] Adjustment | Source |
|---|---|---|---|
| Eu#4 | 0.2743 | 0.978 | From Fig. C-1 |
| Eu#3 | 0.1371 | 0.984 | From Fig. C-1 |
| FTR-$Eu_2O_3$ | 0.324[c] | 0.976 | Interpolated |

a Based on maximum theoretical density.

b Ratio of calculated worth with six mesh intervals to worth with 16 mesh intervals.

c From Fig. 5 - this volume fraction of $Eu_2O_3$ gives the same worth as the FTR-$B_4C$ rod with 1206 grams of $^{10}B$.

References:

1) D.R. Marr, "A User's Manual for 2DBS, A Diffusion Theory Shielding Code," BNWL-1291, Battelle Northwest Laboratory, Richland, WA, February 1970.

## APPENDIX D

## BIAS FACTORS FROM CONTROL ROD INTERACTION STUDY

A set of measured and calculated boron carbide absorber rod worths was obtained from a study of control rod interaction effects[1]. The C/E values from that experiment are given in Table D-I. Using $1/\sigma^2$ weighting, the average C/E is 1.017. The experimental worths were for the withdrawal of safety and control rods from inserted to parked. The calculations were done using constant buckling and four mesh points per subassembly. If the calculated results are adjusted using Fig. C-1 to a mesh spacing equivalent to six mesh intervals per subassembly, the average C/E becomes 1.026. If, in addition, the data are adjusted for axial buckling changes using the factors from the third column of Table IX, the adjusted C/E values, shown in Table D-I, result. The weighted average of the adjusted C/Es is 1.062.

Table D-I

Mesh and Buckling Adjustments to Results of Control Rod Interaction Study

| | C/E[a] | Adjusted C/E[b] |
|---|---|---|
| SR-304 | 0.980 ± .019 | 1.025 ± .020 |
| SR-304 | 1.037 ± .014 | 1.085 ± .015 |
| SR-308 | 1.012 ± .010 | 1.059 ± .011[c] |
| SR-308 | 1.031 ± .014 | 1.079 ± .015 |
| SR-308 | 0.996 ± .021 | 1.043 ± .022 |
| CR-514 | 1.010 ± .015 | 1.054 ± .016 |
| CR-514 | 1.042 ± .015 | 1.087 ± .016[c] |
| CR-514 | 1.069 ± .011 | 1.116 ± .012 |
| CR-516 | 0.997 ± .007 | 1.039 ± .008 |
| CR-516 | 1.001 ± .019 | 1.044 ± .020 |
| CR-516 | 0.967 ± .020 | 1.008 ± .021 |
| CR-516 | 1.032 ± .012 | 1.077 ± .013 |
| Weighted Average | 1.017 | 1.062 |

a From Ref. 1.

b Mesh adjustment = 1.0085 (from four to six mesh intervals) Fig. C-1; buckling adjustment for rod withdrawal (from inserted to parked) Table IX.

c These two measurements correspond to the conditions of the europia worth experiment.

References:

1) J.W. Daughtry, J.F. Meyer and A. Travelli, "Control Rod Interaction Effects in Sodium Cooled Fast Reactors," Proceedings of the Atlanta ANS Topical Meeting on 'Advanced Reactors: Physics, Design and Economics,' (to be published).